J. Membrane Biol. 110, 147–162 (1989)

The Journal of
Membrane Biology

Rabbit Distal Colon Epithelium: I. Isolation and Characterization of Basolateral Plasma Membrane Vesicles from Surface and Crypt Cells

Hubert Wiener†, Klaus Turnheim†, and Carel H. van Os‡
†Department of Pharmacology, University of Vienna, Austria, and ‡Department of Physiology, University of Nijmegen, The Netherlands

Summary. A method has been developed for the simultaneous isolation of basolateral plasma membrane vesicles from surface and crypt cells of rabbit distal colon epithelium by sequential use of differential sedimentation, isopycnic centrifugation and Ficoll 400 barrier centrifugation. The protein yield was high (total 0.81 mg/g mucosa) and surface and crypt cell-derived basolateral membrane fractions have been purified 34- and 9-fold with respect to the homogenate. The pattern of marker enzyme enrichments revealed only minor contamination by subcellular organelles. Latency of ouabain-sensitive (Na^+,K^+)-ATPase activity prior and after trypsin treatment of membranes indicated a vesicle configuration of sealed right side-out : sealed inside-out : leaky of approximately 2 : 1 : 1. The presence of sealed vesicles was also evident from the osmotic sensitivity of the D-[1-^{14}C] mannitol equilibrium space determined with either fraction. Although considerably different in protein profile, surface and crypt basolateral membranes were similar in cholesterol to phospholipid molar ratio and membrane fluidity as determined by steady-state fluorescence polarization.

Stopped-flow light scattering experiments revealed a rather low water permeability of the membranes with a permeability coefficient of 6 μm/sec at 35°C, which is one order of magnitude lower than reported for small intestinal plasma membranes. Both membrane fractions have been shown to effectively generate outward uphill potassium ion gradients, a process that is energized by ATP and inhibited by the membrane-permeant cardiac-glycoside digitoxin. These characteristics are consistent with the activity of a (Na^+,K^+) pump operating in inside-out vesicles.

Key Words rabbit distal colon · surface and crypt cells · basolateral membrane · osmotic water permeability

Introduction

The mammalian colon displays structural [6, 36] and functional [38] heterogeneity: the surface epithelium is involved in electrolyte and fluid absorption, the crypts are thought to be responsible for secretory processes [*reviewed in* 11, 32]. To define the molecular pathways of the transepithelial ion transport, flux studies with purified plasma membrane vesicles has become an attractive methodology [31].

However, the extraction of plasma membrane vesicles from colon epithelium is an intrinsically difficult process, complicated by the structural heterogeneity of the tissue [6, 36] and the presence of mucus, which tends to aggregate membranes, thereby introducing the risk of low yield and arbitrary selection of subsets of vesicles, which may not be representative of the cellular constituent as a whole. Only a few reports are available on the isolation of apical [4, 15, 18, 20, 37] and basolateral [3, 18] plasma membranes of mammalian colon epithelium and only in two studies [20, 37] the vesicle nature of the isolated apical membrane fraction was assessed by transport experiments.

In the present work, rabbit distal colon epithelium was used as a source of biological material since transepithelial ion transport is well characterized by biophysical studies performed on intact epithelia [*cf.* 32, 40]. This is the first report of the isolation of highly purified basolateral membranes of colon epithelial cells, which measures vesicle integrity and membrane sidedness and uses such vesicles for both ATP-dependent "primary active" and ion gradient-coupled "secondary active" ion transport. Additionally, the presented isolation procedure allows the simultaneous preparation of basolateral membrane vesicles from surface and crypt epithelial cells. Currently, ion transport studies using plasma membrane vesicles seem to be a promising experimental approach to get insight into molecular aspects and regulatory parameters of basolateral ion transport in colon epithelial cells since electrophysiological studies are hampered by technical difficulties [42] inherent to this tissue.

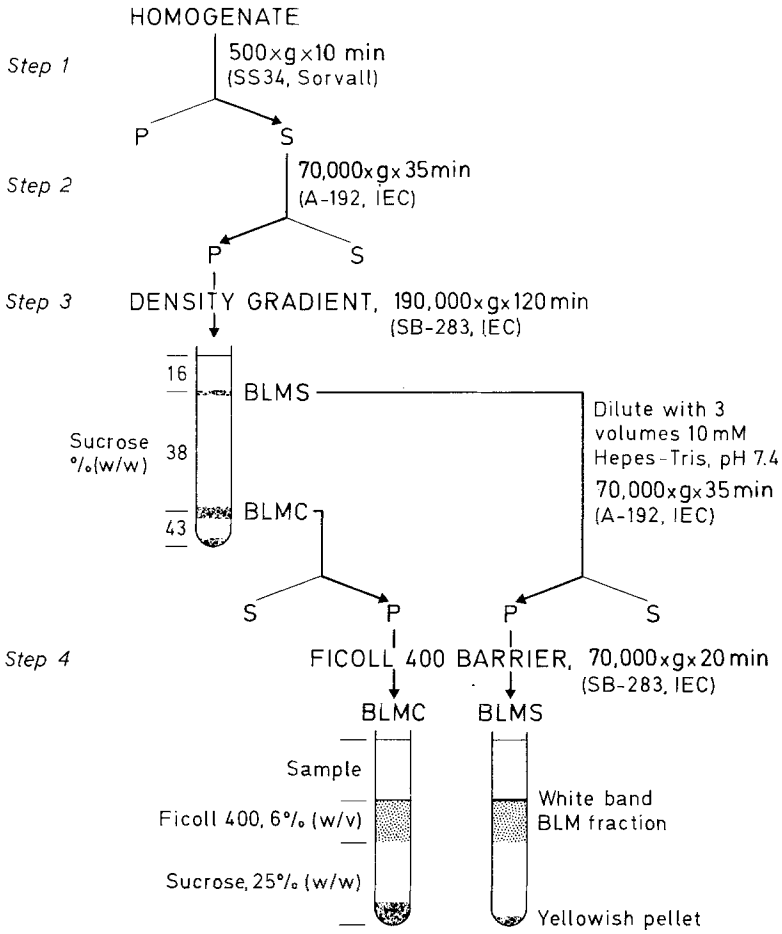

Fig. 1. Flow scheme for the preparation of basolateral plasma membrane vesicles from rabbit distal colon epithelium

Materials and Methods

Isolation of Rabbit Colon Basolateral Membrane Vesicles

New Zealand white rabbits (either sex, ≈2.5 kg weight) maintained on standardized commercial diets were killed by cervical dislocation and bled. The distal colon (≈40 cm in length) was rapidly dissected, cut into ≈8 cm pieces, which were flushed immediately with ice-cold 0.9% NaCl to remove fecal contents, and placed on ice. The segments were then opened along their length, spread luminal surface uppermost on a 150-mm diameter glass petri dish placed bottom-up on ice, and were cleaned thoroughly with gauze to remove mucus and adhering material. The colon mucosa was harvested by gently scraping with glass slides. Typically, the preparation began with 6–8 g (wet wt) of scrapings obtained from two rabbits. The scrapings were minced with scissors, suspended (≤3% wet/vol) in ice-cold 250 mM sucrose, 25 mM choline chloride, 1 mM dithiothreitol, 0.2 mM phenylmethylsulfonyl fluoride, 5 mM HEPES-Tris, pH 8.3, and homogenized for 15 min at 40% of maximum speed (9500 rpm) in a Bühler homogenizer. The homogenization was performed in 85-ml portions using the 150-ml blending chamber cooled by a layer of ice slush kept around the homogenization cylinder. May-Grünwald-Giemsa stained smears of the homogenate showed that this procedure breaks most (>90% on the basis of recognizable particle count) of the epithelial cells with only moderate damaging effects on nuclei. Minor nonepithelial contaminants (connective tissue, smooth muscle cells) of the scrapings remain intact.

High-speed centrifugation steps were performed at 3°C and run parameters are given in terms of g_{av}, where g_{av} is the centrifugal force (times gravity) at the average radial distance, i.e., the mean between maximum (tube bottom) and minimum (meniscus) distance from the axis of rotation. Density gradients were constructed of sorbitol or sucrose buffered with 10 mM HEPES-Tris, pH 7.4; concentrations of solutes are given as percent by weight (Fig. 1).

Step 1. The homogenates were combined and subjected to low-speed differential sedimentation (Sorvall, SS34 rotor) at 500 × g × 10 min. The supernatants containing soluble protein and the crude membrane fraction were carefully decanted, pooled, and further processed in step 2. The pellets containing ≈10% of total protein (gross cell debris, unbroken nonepithelial elements, nuclei, and some aggregating particulate material as judged by light microscopy and diagnostic marker enzymes) were discarded (Table 1; Fig. 1).

Step 2. The low-speed supernatant obtained at step 1 was then separated by centrifugation for 35 min at 70,000 × g into a soluble (supernatant) fraction, which was discarded, and a sedimentable (pellet) crude membrane fraction, which was further subfractionated by isopycnic centrifugation in step 3 (Fig. 1).

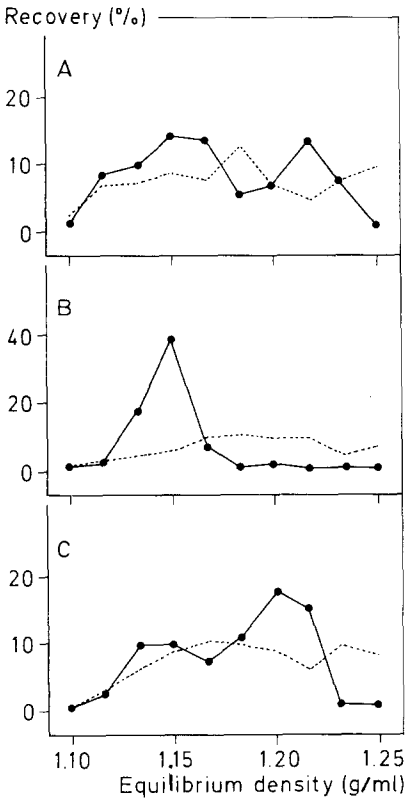

Fig. 2. Analytical subfractionation of epithelial cell membranes of rabbit distal colon. Representative (out of three to six separate fractionations) density distribution pattern of (Na^+,K^+)-ATPase (solid line) and protein (dotted line) after fractionation of (*A*) mucosal scrapings, (*B*) surface cells, and (*C*) mucosal scrapings after removal of surface cells, on continuous linear sorbitol gradients. For experimental details *see* Materials and Methods. Marker recovery after centrifugation is plotted as a function of equilibrium density. Total recoveries after centrifugation: protein, 87%; and (Na^+,K^+)-ATPase, 84%, of the applied quantities

Step 3. The crude membranes were resuspended at 5–10 mg protein/ml in 250 mM sucrose, 5 mM HEPES-Tris, pH 7.4, by 40 strokes with a loose fitting (pestle A) Dounce homogenizer (Kontes Glass, Vineland, NJ). For analytical subfractionation (Fig. 2), continuous linear density gradients were loaded with the crude membrane suspension at a sample volume of 0.05 units of gradient bed volume and centrifuged for 14 hr at 75,000 × *g*. Fractions were removed from the top of the gradient with a Buchler Auto Densi-Flow (Buchler Instruments, Fort Lee, NJ), and the density of each fraction was determined gravimetrically. Each fraction was then diluted with ≈4 volumes of gradient buffer, and sedimented for 25 min at 170,000 × *g*. The pellets were resuspended in minimal volumes (100–300 μl) of 250 mM sucrose, 10 mM HEPES-Tris, pH 7.4, by repeated passage through a No. 25 gauge needle.

Preparative subfractionations (Fig. 1) were usually performed in runs at 40,000 rpm for 2 hr (190,000 × *g*) with tubes each containing 3 ml 16% sucrose, 6 ml of the crude membrane fraction, which was made 38% in sucrose (final protein ≈2.5 mg/ml), and 2 ml 43% sucrose cushion. Similar results were obtained with step gradients of 8 ml 16% sucrose, 25 ml 38% sucrose containing the crude membrane fraction, 6 ml 43% sucrose cushion spun 14 hr at 75,000 × *g*, BLMS (basolateral membranes referred to surface epithelial cells) and BLMC (basolateral membranes referred to crypt epithelial cells) fractions collecting at the 16/38% and 38/43% sucrose interface, respectively, were harvested separately by quantitative aspiration of the individual bands. The membrane fractions were then diluted ≈ threefold in gradient buffer, and recovered at 70,000 × *g* for 35 min. The pellets were resuspended at 3–5 mg protein/ml in 250 mM sucrose, 10 mM HEPES-Tris, pH 7.4, by 20 gentle strokes with pestle A in a Dounce homogenizer (Fig. 1).

Step 4. The basolateral membranes were purified further by Ficoll 400 barrier fractionation at 70,000 × *g* at the sample/barrier interface for 20 min (Fig. 1). Each tube contained 3-ml sample layer, 2 ml 6% (wt/vol) Ficoll 400 in 250 mM sucrose, 5 mM HEPES-Tris, pH 7.4, and a 5-ml cushion of 25% sucrose. After centrifugation the 3-ml sample layer and a small band at the sample/Ficoll interface containing subcellular membranes (endoplasmic reticulum, Golgi membranes as judged by marker enzyme analysis) were discarded. The highly purified BLMS and BLMC fractions trapped within the Ficoll barrier were collected, pooled separately, diluted five- to 10-fold with medium, which varied according to the experimental design and sedimented at 70,000 × *g* for 35 min. The pellets were resuspended in the same medium to 12–15 mg protein/ml by repeated passage through a No. 25 gauge needle. Aliquots were frozen in liquid nitrogen and stored at −80°C.

Enzyme Assays

Assays were corrected for nonenzymatic reaction rate, were linear functions of protein and time, and were carried out on samples, which were either freshly prepared or frozen and thawed only once. (Na^+,K^+)-ATPase activity was measured at 37°C as the rate of inorganic phosphate release in the slightly modified medium of Mircheff et al. [25] containing 100 mM NaCl, 10 mM KCl, 5 mM $MgCl_2$, 2.9 mM EDTA, 2 mM Na_2ATP, 50 mM Tris-Cl, pH 7.4, in the absence and presence of 1 mM ouabain; final volume 0.5 ml. The reaction was initiated by the addition of protein. Unless otherwise stated, membrane vesicles were pretreated with detergent to ensure full access of substrates to both sides of membranes (*see below*). The addition of 0.5 ml ice-cold 5% (wt/vol) trichloroacetic acid terminated the reaction. Aliquots were used directly for phosphate determination except when samples contained >5 μg of protein, which were first centrifuged to remove precipitated protein. Ouabain-sensitive ATP hydrolysis was in the range of 2.5 to 24% of the total ATP hydrolysis. Other enzyme activities were assayed according to published methods, modified as indicated: ouabain-insensitive (K^+) phosphatase [15]; acid phosphatase [23] in the presence of 4 mM EDTA to inhibit alkaline phosphatase [17]; alkaline phosphatase [25], except that $ZnCl_2$ was omitted from the assay mixture; succinate dehydrogenase [26] as modified by [28]; NADH- and NADPH-cytochrome *c* reductase [35] using a molar absorption coefficient of $\varepsilon = 19.6 \times 10^3\ M^{-1}\ cm^{-1}$ [44] for the reduced minus the oxidized cytochrome. Thiamine pyrophosphatase [22] with the modification that 2 mM theophylline was included to inhibit alkaline phosphatase activity.

Analysis of Membrane Sidedness and Integrity

Methodology used is based on latency [*cf.* 19] and site-specific trypsin sensitivity [10] of plasma membrane (Na^+,K^+)-ATPase. In order to expose latent enzyme activity in trypsin-treated and

untreated membranes, samples were suspended at 1 mg protein/ml in 250 mM sucrose, 10 mM HEPES-Tris, pH 7.4 and pretreated with varying concentrations of, (*i*) Triton X-100/digitonin 1:1 (wt/wt) for 20 min on ice, (*ii*) SDS for 5 min on ice, (*iii*) the channel-forming antibiotic alamethicin for 20 min at room temperature, or (*iv*) by osmotic shock (≥50-fold dilution of membranes in distilled water), before diluting aliquots into the (Na^+,K^+)-ATPase assay medium. Experimental details of trypsin treatment of membranes are described in the legend to Fig. 7. Complete sidedness information can be extracted from ouabain-sensitive (Na^+,K^+)-ATPase activity in the absence (*a*) and presence (*b*) of detergent in trypsin-untreated membranes and from activity in the presence (*c*) of detergent in trypsin-treated (10 min) membranes: (*a*/*b*), leaky vesicles; [(*b* − *a*)/*b*], sealed both right side-out and inside-out vesicles. Percentage of sealed inside-out vesicles can be calculated by difference from the total percentage of sealed vesicles.

Chemical Analysis

Inorganic phosphate released by phosphatase activity was quantified colorimetrically [2]. To minimize interference by thiols [43] and nonionic detergents [30], the concentrations of dithiothreitol and Triton X-100 in the final assay mixture were limited to 0.02 mM and 0.025 mg/ml, respectively. At this concentration, the effect on standard curves was negligible.

Membrane lipids were extracted by a modified procedure [8] of the method of Folch, Lees and Stanley [9], except that dichloromethan/methanol (2:1, vol/vol) was used as an extraction medium. Total phospholipid phosphate [5] and total cholesterol [1] (using kit no. 351, Sigma, St. Louis) were determined by the indicated published methods. The phospholipid/protein ratio on a wt/wt basis was estimated assuming a mean phospholipid mol wt of 770.

Protein was estimated by the Biorad assay based on Coomassie blue G-250 dye binding using gamma-globulin as standard. Samples were prepared in the presence of Triton X-100 (0.1%, vol/vol) to promote rapid solubilization of membrane proteins. In samples of BLMS and BLMC treated with Triton, the amount of total protein was ≈40 and ≈10% higher than in untreated samples.

Protein analysis of membrane fractions was carried out by SDS-polyacrylamide slab gel electrophoresis [21] as described elsewhere [39].

Light Scattering

Scattered light intensity was measured at a wavelength of 450 nm 90° to the incident beam using an Aminco Morrow stopped-flow system mounted on an Aminco DW2a spectrophotometer. Membrane suspensions in 100 mM mannitol, 2 mM $MgCl_2$, 5 mM HEPES-Tris, pH 7.4, were rapidly mixed (4 atm pressure) with equal volumes of hyper- or isosmotic solutions, and changes in light scatter intensity were recorded and signal-averaged in an Aminco Midan T microprocessor-data-analyzer. The osmotic water permeability coefficient, P_f, was calculated [16] from:

$$P_f = \frac{K}{C_m} \cdot \frac{1}{V_w} \cdot \frac{V_o}{A}\left(1 - \frac{b}{V_o}\right) \quad (1)$$

where K is the rate constant of osmotic water permeation, C_m is the osmolarity of the external solution, V_w is the molar water volume, and V_o (vesicular volume), A (vesicular surface area), and b (osmotically inactive vesicle volume) are dimensional parameters estimated stereologically from electron micrographs (*see* Fig. 4). The rate constant K was obtained from first-order plots of the time course data shown in Fig. 9.

Electron Microscopy

Transmission electron micrographs were kindly prepared by M. Pavelka (Department of Micromorphology and Electronmicroscopy, University of Vienna). Membrane pellets obtained after the final purification step (*see* isolation procedure) were fixed in ice-cold 250 mM sucrose, 2.5% glutaraldehyde, 100 mM cacodylate, pH 7.4, overnight in the cold, and, thereafter, washed to remove the glutaraldehyde, postfixed in 1% veronal acetate-buffered OsO_4, dehydrated in graded ethanol solutions, and embedded in Epon. Ultrathin sections were stained with uranyl acetate-lead citrate and examined on a Philips EM400 electron microscope. Randomly chosen vesicular structures from representative fields of the thin section transmission electron micrographs were stereologically analyzed on a desk computer (Video-plan, Kontron Gmbh, FRG).

Fluorescence Polarization

Aliquots of final purified membrane suspensions were diluted (final concentrations 25 to 50 μg protein/ml) into 150 mM NaCl, 2 μM 1,6-diphenyl-1,3,5-hexatriene, 1% (vol/vol) ethanol, 20 mM HEPES-Tris, pH 7.4, and incubated in the dark for 30 min at 37°C. Fluorescence emission intensities (excitation wavelength 370 nm, emission wavelength 430 nm) were recorded parallel ($I_\parallel$) and perpendicular ($I_\perp$) to the exciting plane on an Aminco-Bowman spectrofluorometer thermostated at 37°C. Steady-state fluorescence anisotropy $r = (I_\parallel - I_\perp)/(I_\parallel + 2I_\perp)$ was determined at different protein concentrations and extrapolated to zero dilution to correct for emission scattering. The anisotropy parameter $(r_o/r - 1)^{-1}$ was calculated assuming a maximal limiting anisotropy of 1,6-diphenyl-1,3,5-hexatriene of $r_o = 0.362$ [34].

Radionuclide Transport Studies

^{86}Rb, which can substitute for potassium in activation of (Na^+,K^+)-ATPase [19] was used as a tracer to measure ATP-dependent potassium uphill transport mediated by (Na^+,K^+)-antiport. A protocol similar to that of Seiler and Fleischer [33] was used.

After ion equilibration of membrane vesicles in 5 mM NaCl, 50 mM KCl, 5 mM $MgCl_2$, 2.9 mM EDTA, 5 mM phosphoenolpyruvate, 32 U/ml pyruvatekinase, 50 mM Tris-HCl, pH 7.4, 3.5×10^6 cpm/ml ^{86}Rb for 3 hr on ice and 30-min temperature equilibration at 25°C, active transport was initiated by the addition of 3 mM Tris-ATP. Controls were performed in the absence of ATP. Transport was terminated at appropriate time intervals by rapid filtration of 0.5 ml aliquots (containing 50 μg of protein) through prewetted filters (0.45 μm ME 25 filter, Schleicher & Schüll, Dassel, FRG). The filters were washed two times with 2.5 ml washes of stop solution (ice-cold 0.5 M KCl, 10 mM Tris-NCl) and placed in glass vials containing 8 ml of Ready-Solv HP scintillation fluid (Beckman, Fullerton, CA). Radioactivity was measured by scintillation spectrometry. All values were corrected for blank, i.e., radioactivity retained on the filter in the absence of protein.

Table 1. Influence of homogenization medium on the yield of sealed plasma membrane vesicles[a]

Condition	Homogenate			Subfractions recovery[c] (%)		
	−Detergent [*a*]	+Detergent[b] [*b*]	Latency (%) [(*b* − *a*)/*b*]	*P*	*S*	Total
pH 6.5	0.86 ± 0.6	1.19 ± 0.2 (6)	28	48 ± 5	61 ± 8	109 ± 7 (3)
pH 7.3	0.87 ± 0.3	1.33 ± 0.3 (5)	35	24 ± 3	82 ± 16	106 ± 18 (3)
pH 8.3	0.82 ± 0.4	1.27 ± 0.3 (7)	35	6 ± 0.4	93 ± 9	99 ± 9 (3)
+ NaCl (25 mM)	0.64 ± 0.2	1.26 ± 0.2 (6)	49	22 ± 4	77 ± 5	99 ± 2 (5)
+ Choline Cl (25 mM)	0.56 ± 0.1	1.25 ± 0.2 (6)	55	9 ± 5	87 ± 10	96 ± 7 (5)

[a] Mucosal scrapings were homogenized in 250 mM sucrose, 1 mM dithiothreitol, 0.2 mM phenylmethylsulfonyl fluoride, 10 mM of either Mes-Tris, pH 6.5, HEPES-Tris, pH 7.3, or Tris-HEPES, pH 8.3, and the indicated additions, stored on ice for 15 min, and subjected to low-speed centrifugation (step 1, Fig. 3). The crude homogenate, the pellet (*P*) and the supernatant (*S*) fraction were analyzed for (Na^+,K^+)-ATPase activity in the presence and absence of detergent. Other details as described under Materials and Methods. Values are mean ± SD of *n* different preparations shown in parentheses.

[b] Triton X-100/digitonin 1 : 1 (wt/wt), 0.4 mg detergent per 1 mg of protein.

[c] Relative to the amount in the homogenate.

Total trapped volume in a vesicle suspension was measured by isotope equilibrium uptake. Final purified membranes were prepared in 150 mM KCl, 10 mM $MgCl_2$, 20 mM HEPES-Tris, pH 7.4, temperature equilibrated for 15 min at 25°C, and diluted to 1 mg protein/ml into an identical medium containing 1.6×10^6 cpm/ml of D-[1-^{14}C] mannitol. The external medium osmolarity was varied by addition of raffinose. After 90 min, incubation aliquots of incubate were diluted 20-fold into ice-cold stop solution (uptake medium containing 1 mM unlabeled mannitol instead of radioactive tracer), filtered, washed twice with 2 ml stop solution and processed for scintillation counting as described above. Linear regression analysis of apparent equilibrium space *vs.* inverse medium osmolarity yield average trapped volumes at isosmotic (0.35 osM) conditions corrected for trapping of the label in an osmotically inactive space.

Materials

All enzymatic substrates, ouabain, digitoxin, valinomycin, phenylmethylsulfonyl fluoride, 1,6-diphenyl-1,3,5-hexatriene, digitonin, Triton X-100, porcine trypsin (EC 3.4.21.4, Sigma T-0134) and soybean trypsin inhibitor were obtained from Sigma (St. Louis, MO). Alamethicin (stock solution, 30 mg/ml in ethanol) was kindly provided by Richard L. Keene (Upjohn, Kalamazoo, MI). Theophylline was from ICN Pharmaceuticals (Plainview, NY), pyruvate kinase (EC 2.7.1.40) from Boehringer (Mannheim, FRG) and Ficoll 400 from Pharmacia (Uppsala, Sweden). Gel electrophoresis reagents were obtained from Bio Rad (Richmond, CA), D-[1-^{14}C] mannitol (55 mCi/mmol) was purchased from Amersham and ^{86}Rb from New England Nuclear. All other chemicals were reagent grade.

Results

Isolation of Basolateral Plasma Membrane Vesicles

Initially, homogenization and low speed centrifugation (step 1) was troublesome. Aggregation of membrane material resulted in high losses in pellet P. The problem could be solved by increasing the pH of the homogenization medium to 8.3 (Table 1). In addition, the resealing of basolateral membrane vesicles could be substantially improved by adding 25 mM choline Cl to this medium. Surprisingly, NaCl was less effective than choline Cl and the pH was not of influence on resealing (Table 1).

In other initial experiments, density profile of subcellular membrane fractions of rabbit distal colon epithelium was established by analytical subfractionation on a continuous linear density gradient. Three sources of biological material were used: (*i*) mucosal scrapings, (*ii*) isolated surface cells, and (*iii*) scrapings after removal of the surface cell layer, i.e., predominantly colonic crypts. We applied the established procedure of Gustin and Goodman [15] for isolation of rabbit colon epithelial cells combining mechanical dissociation with chelation of divalent cations. The protein content of the isolated cells was roughly 1.9×10^{-7} mg of protein per single cell. Under the conditions used, 2 hr harvesting yielded about 0.5×10^8 dissociated cells per 10 cm length of colon. However, the most notable feature of the cumulative marker recovery profile shown in Fig. 3 was that 75% of the mitochondrial marker succinate dehydrogenase and approximately 60% of total (Na^+,K^+)-ATPase activity are recovered in dissociated cells equivalent to only 35% of the total amount of protein. The remainder of constituents is tightly associated with the mucosa and can be harvested by scraping. This enzyme pattern of dissociated cells indicates a high mitochondrial density and a high (Na^+,K^+)-ATPase content as expected for surface epithelial cells, which are known to be involved predominantly in Na^+ absorption [32]. The origin of isolated cells was further evaluated by histological examination (*not shown*) of mucosal scrap-

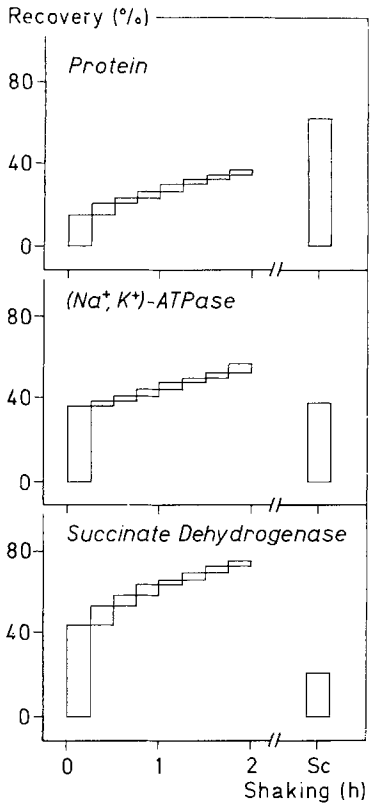

Fig. 3. Isolation of rabbit distal colon epithelial cells. Epithelial cells were dissociated by shaking everted colon sacs in 200 ml volumes of 5 mM EDTA, 30 mM NaCl, 1 mM dithiothreitol, 8 mM HEPES-Tris, pH 7.6, at 6°C as described previously [8]. Cells were collected in 15-min intervals by centrifugation (330 × *g* × 10 min) homogenized, and analyzed for biochemical constituents. For details *see* Materials and Methods. Cummulative recovery of constituents is expressed as the percent of total amount (cell suspensions plus, S_c, scrapings of the remaining epithelium after harvesting cells for 2 hr) of constituent per 10 cm of colon: protein, 28 mg; (Na^+,K^+)-ATPase, 36 μmol P_i/hr; succinate dehydrogenase, 8 μmol/hr

ings before and after harvesting cells. Crypts were left intact by the cell isolation procedure whereas the surface area of the mucosa was largely denuded of epithelial cells.

Crypt cells can thus be harvested by scraping the mucosal layer after dissociating the majority of surface cells according to Gustin and Goodman [15].

In Fig. 2, we present the density distribution of basolateral plasma membranes represented by (Na^+,K^+)-ATPase activity after fractionation of scrapings and compare it with that observed with isolated surface cells and scrapings after removal of the surface cell layer. The pattern obtained with mucosal scrapings (Fig. 2*A*) revealed that (Na^+,K^+)-ATPase activity equilibrates in two peaks with ≈2/3 of the total activity recovered at density <1.16, the peak fraction centered at 1.145 (range 1.135–1.15 with six preparations), and with ≈1/3 of activity recovered at density >1.16 with a peak near 1.195 (range 1.17–1.22 in six preparations). The latter portion of activity, however, was not found when membranes of surface cells were fractionated (Fig. 2*B*). (Na^+,K^+)-ATPase activity with these membranes showed a rather symmetrical peak with a mode at density 1.15, a position corresponding to the low density peak obtained by fractionation of scrapings (*see above*). This coincidence in peak position indicates that the low density peak of (Na^+,K^+)-ATPase activity in the distribution pattern of scrapings apparently originates from basolateral membranes of surface cells. On the other hand, when colonic crypts, i.e., mucosal scrapings, after removal of the surface cell layer, were fractionated (Fig. 2*C*) again a bimodal (Na^+,K^+)-ATPase distribution was found on the density gradient. Although the peak positions are comparable to those obtained with scrapings of total epithelium, the peak ratio is different due to a considerably higher quantity of membranes equilibrating in the high density (>1.16) region. This is suggestive evidence that the high density peak of (Na^+,K^+)-ATPase activity apparently contributes to basolateral plasma membranes of cells originating from the crypt region. The smaller quantity being equilibrated in the low density region may reflect contamination by surface cells. However, this initial observation that basolateral plasma membranes of crypt cells seem to be centered at distinctly higher density than that of surface cells provided the rationale for the preparative fractionation procedure presented in Fig. 1. Mucosal scrapings were homogenized and a crude membrane fraction was prepared by differential sedimentation. Basolateral membranes of surface (BLMS) and crypt (BLMC) cells were separated by isopycnic centrifugation using a sucrose density step gradient and further purified by Ficoll 400 barrier centrifugation. In Table 2, the isolation profile is shown with the yield and purification factors of both basolateral membrane preparations.

The degree of purification for the final membrane fraction was assessed via the specific activi ties of conventional marker enzymes [e.g., 15, 24 37] for basolateral plasma membranes ((Na^+,K^+) ATPase), apical plasma membranes (ouabain-insen sitive (K^+) phosphatase, alkaline phosphatase) Golgi membranes (thiamine pyrophosphatase), mitochondria (succinate dehydrogenase), lysosomes (acid phosphatase) and endoplasmic reticulum (NADPH- and NADH cytochrome *c* reductase). Although several of the markers used are associated with more than one membrane population [24], the pattern of marker activities presented in Table 3

Table 2. Preparative isolation profile of basolateral membranes from rabbit descending colon epithelium[a]

Isolation step	Total protein[b] (mg/7 g of scraping)	(Na^+,K^+)-ATPase[c] (μmol P_i/mg · hr)	Yield[d] (%)	Enrichment (fold)
Homogenate	686	1.27 (0.4)		1
Step 1	620	1.38 (0.4)	98	1.1
Step 2	203	3.45 (0.4)	82	2.6
Step 3				
16/38% interface	22	20 (0.8)	63	16
38/43% interface	63	1.5 (0.5)	13	1.1
Step 4				
BLMS	3.4	43 (0.8)	33	34[e]
BLMC	2.0	11 (0.5)	23	9[f]

[a] The isolation procedure was monitored with (Na^+,K^+)-ATPase as plasma membrane marker. Values are the mean of multiple determinations from seven different batches of membranes.
[b] Normalized per 7 g (wet wt) of mucosal scrapings, which is the average mass obtained from two rabbits.
[c] Measured after preincubation in Triton X-100/digitonin 1 : 1 (wt/wt) (*see* Fig. 6); the optimum detergent concentration used (mg detergent per 1 mg of protein) is given in parentheses.
[d] With respect to the preceding step.
[e] 34 ± 6-fold (mean ± SD, range 25- to 44-fold).
[f] 9 ± 2-fold (mean ± SD, range 5.6- to 12.2-fold).

gives an idea of the heterogeneity of the membranes. Of the three plasma membrane marker enzymes used, (Na^+,K^+)-ATPase gave the highest purification indicating a substantial enrichment in basolateral membranes. Highly purified apical plasma membranes of rabbit distal colon epithelium have a ouabain-insensitive (K^+) phosphatase activity of 12.5 μmol/mg · hr [15]. Using this value and a specific activity of 0.5 and 0.3 μmol/mg · hr in the BLMS and BLMC fraction, an upper limit of apical membrane contamination can be estimated at 4 and 2.4%, respectively. An eight- and 4.5-fold (BLMS *vs.* BLMC) purification was also observed with alkaline phosphatase as an apical plasma membrane marker. However, the ≈threefold higher enrichment compared to ouabain-insensitive (K^+) phosphatase may be due to its presence in both apical and nonapical membranes of rabbit distal colon epithelial cells [37]. A nominal amount of contamination was present from endoplasmic reticulum, Golgi membranes and lysosomes, as indicated by the low (≤3.3-fold) enrichment of the corresponding markers. The mitochondrial marker succinate dehydrogenase was not significantly enriched in the membrane fraction compared to the homogenate. Total marker and protein recoveries during various purification steps ranged from 66 to 110%.

Transmission electron micrographs representative of BLMS, Fig. 4, showed the membrane preparations consisted predominantly of irregular-shaped vesicular structures with little visible internal filamentous content (presumably remnants of the cytoskeleton). Statistical size analysis gave a roughly bell-shaped size distribution histogram (inset in Fig. 4) with a mean diameter of the predominant vesicle population of 0.2 μm. Examination of micrographs of several representative sections (covering a total area of ≈550 μm^2) of this fraction revealed only minor contamination with remnants of ribosomes, mitochondria and lysosomes, and a background of amorphous material and unidentifiable membranes and debris. This background contamination with subcellular organelles confirms the distribution pattern of marker enzymes discussed above.

Plasma Membrane Parameters

The total phospholipid content is ≈fourfold greater in the BLMS fraction (Table 4), in the same proportion as other vesicle characteristics (*see below*). However, the cholesterol/phospholipid molar ratios, although slightly lower in the BLMC fraction are comparable for both BLMS and BLMC (0.69 *vs.* 0.56).

The fluidity of the membrane lipid matrix was evaluated by steady-state fluorescence polarization with 1,6-diphenyl-1,3,5-hexatriene as fluorophore. Comparison of anisotropy data (Table 4) implied that at 37°C the motion of the fluorophore in the BLMS fraction showed slightly greater restriction (r = 0.195), indicating that the overall membrane fluidity is somewhat lower than in the BLMC (r = 0.185) fraction. The lower fluidity of BLMS corre-

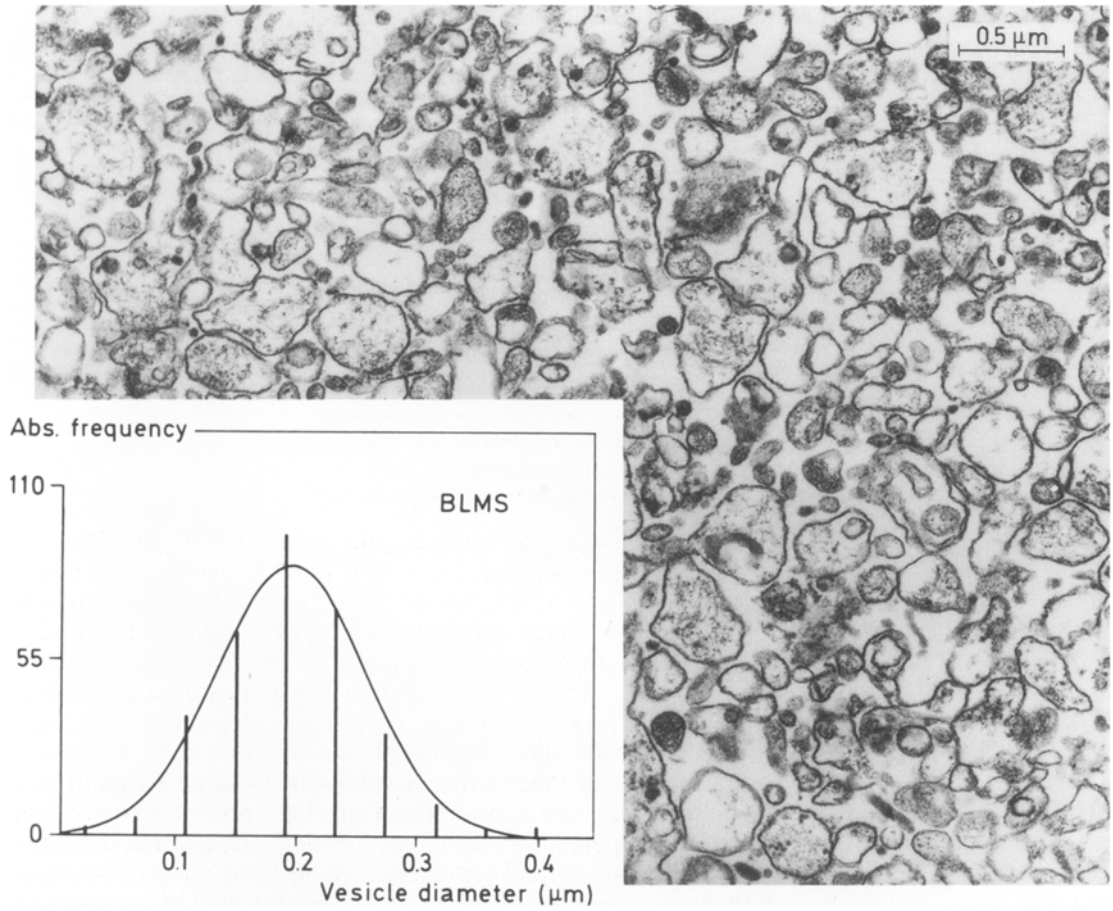

Fig. 4. Transmission electron micrograph of basolateral membranes from rabbit distal colon epithelium. The final purified BLMS fraction was processed for electron microscopy as described under Materials and Methods. The micrograph shows a uniform membrane profile of irregular-shaped vesicles of various sizes (bar, 0.5 μm; original magnification, 13,500×). Inset, size distribution histogram of vesicles with Gaussian distribution (dotted line) around the mean value (±SD) of 0.195 ± 0.062 μm, n = 324

lates well with the higher cholesterol/phospholipid ratio.

The protein profiles of the isolated membrane fractions were compared by SDS-polyacrylamide gel electrophoresis (Fig. 5). The gel pattern of BLMS is distinctly different from those of BLMC in a variety of polypeptides of different molecular weights. However, some proteins found may represent soluble protein simply trapped inside the vesicles during their preparation and may also be polypeptides originating from some filamentous material co-purifying with the membrane vesicles. Indeed, the intense 43-kDa band in the slab gels could arise at least in part from actin [12]. The concentration of soluble protein is ≈2.3 mg/ml (supernatant in step 2 of the isolation procedure). Assuming the same concentration inside the vesicles and a vesicular volume of ≤0.91 μl/mg protein (*see below*) the soluble protein trapped within vesicles should be <0.3% of total protein.

Both membrane fractions show a significantly different relative intensity of bands compared with the crude membrane fraction. Most notably, in the BLMS the enrichment of 95- and 38-kDa bands, assumed to refer to the α- and β-subunit of (Na^+,K^+)-ATPase [19], seems to reflect the high purification factor observed for (Na^+,K^+)-ATPase. In BLMC, however, the same bands are not distinctly darker than in crude membranes.

Membrane Sidedness and Integrity of Vesicles

Generally, the isolated plasma membranes can be represented as (*i*) sealed right side-out vesicles, oriented with their extracellular face exposed, (*ii*) sealed inside-out vesicles, oriented with their cytoplasmic face exposed, and (*iii*) leaky vesicles and broken membranes with both faces exposed. Meth-

Table 3. Enzyme marker activities of purified membrane fractions[a]

Enzyme marker	Homogenate	BLMS		BLMC	
	Specific activity (μmol/mg · hr)	Yield (%)	Enrichment (fold)	Yield (%)	Enrichment (fold)
Na^+,K^+-ATPase[b]	1.27 ± 0.2	16.7	34	2.5	9
Alkaline phosphatase	0.4 ± 0.1	3.3	8	1.4	4.5
Ouabain-insensitive (K^+) phosphatase	0.2 ± 0.1	1.0	2.5	0.5	1.5
Acid phosphatase	2.4 ± 1	0.8	2.2	0.4	1.4
Thiamine pyrophosphatase	0.24 ± 0.2	1.1	3.3	0.8	2.8
NADPH-cytochrome *c* reductase	0.04 ± 0.01	0.5	1.5	0.7	2.3
NADH-cytochrome *c* reductase	0.5 ± 0.1	0.6	1.6	0.6	2.0
Succinate dehydrogenase	0.3 ± 0.1	0.3	0.7	0.4	1.3

[a] Values are the mean ± SD of replicate determinations from three to 10 different batches of membranes.
[b] Measured after detergent pretreatment (*see* Fig. 6).

Table 4. Properties of isolated membrane vesicles[a]

Property	BLMS	BLMC
Total phospholipid (nmol/mg protein)	213 ± 19 (4)	52 ± 10 (4)
Cholesterol (nmol/mg protein)	146 ± 8 (4)	29 ± 7 (4)
Cholesterol/phospholipid (molar ratio)	0.69	0.56
Membrane fluidity[b], 37°C		
Fluorescence anisotropy	0.195 (2)	0.185 (2)
Anisotropy parameter	1.17	1.05
Osmotic water permeation[c], 35°C		
Rate constant (sec^{-1})	2.39	2.69
Permeability coefficient (μm/sec)	6.1	ND
Trapped volume[d] (μl/mg protein)	0.91	0.24
Dimensional parameters[e]		
Mean vesicle diameter (μm)	0.195	ND
Vesicle surface area (μm^2)	0.12	ND
Vesicular volume (μm^3)	0.0039	ND

[a] The data represent the mean ± SD with the numbers of preparations analyzed given in parentheses.
[b] Determined by steady-state fluorescence polarization of 1,6-diphenyl-1,3,5-hexatriene.
[c] Measured by stopped-flow light scattering (*see* Fig. 9).
[d] Determined from D-[1-^{14}C] mannitol equilibrium space (*see* Fig. 8).
[e] Estimated stereologically from electron micrographs (*see* Fig. 4).

odology using (Na^+,K^+)-ATPase activity to quantify these different membrane configurations is based on the following two assumptions. First, ouabain-sensitive (Na^+,K^+)-ATPase cannot be measured in sealed vesicles regardless of membrane orientation since ATP and ouabain bind to opposite membrane faces of this transmembrane pump [for review *see* 19]. When latency is removed by leak producing agents, any increase in ouabain-sensitive (Na^+,K^+)-ATPase activity is referable to sealed vesicles both right side-out and inside-out. The second assumption is that (Na^+,K^+)-ATPase is sensitive to trypsin from the cytoplasmic face, but not from the extracellular face of the plasma membrane [13]. Consequently, any increment of activity exposed by leak-producing agents following trypsin treatment of membranes is a measure of right side-out vesicles [10].

Two further premises are implicit in that methodology. The first is that ouabain [14] is excluded from the interior of sealed vesicles, at the levels used for the (Na^+,K^+)-ATPase assay. This assumption seems to be valid for both BLMS and BLMC since ATP hydrolysis in the presence of 1 mM ouabain was linear with time for at least 10 min (*not shown*). Permeation of ouabain into the vesicles during incubation would result in progressive decrease in ATP hydrolysis as a function of time. The second premise is that increase of ouabain-sensitive (Na^+,K^+)-ATPase activity reflects lysis or rupture of membrane vesicles making binding entities accessible to ligands. However, increment of activity by detergents could be the net effect of both disruption of the membrane barrier and direct action on the (Na^+,K^+)-ATPase molecule, which can be activatory and/or inhibitory in a concentration dependent manner [19], thereby introducing inaccuracies in quantification of sealed vesicles. Indeed, as seen in Fig. 6, the enzyme activity decline when excess detergent was used in the preincubation medium. It should also be noted that the optimal detergent concentration giving maximal (Na^+,K^+)-ATPase activity depended on the purity of the sample being assayed. It was ≈0.4 mg of Triton X-100/digitonin 1 : 1 (wt/wt) per mg of protein for the crude membrane fractions and 0.8 and 0.5 mg detergent per mg of protein for the final purified BLMS and BLMC fraction, respectively. Apparently, the increased optimal detergent concentration parallels the increased

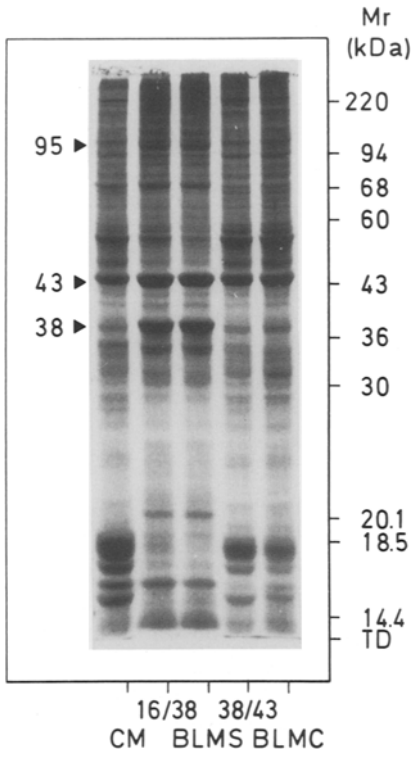

Fig. 5. SDS-polyacrylamide slab gel electrophoresis of purified membrane fractions. Aliquots (20 μg of protein) of crude membranes, CM, (step 2), semipurified basolateral membranes (step 3; 16/38% and 38/43% interface) and final (step 4) purified BLMS and BLMC were subjected to electrophoresis on a SDS/12.5% polyacrylamide gel and stained with coomassie blue GI-250. Apparent molecular weight values were estimated by reference to a curve of relative mobility *vs.* log (M_r) using ferritin (220 kDa), phosphorylase *b* (94 kDa), albumin (68 kDa), catalase (60 kDa), ovalbumin (43 kDa), lactat dehydrogenase (36 kDa), carbonic anhydrase (30 kDa), trypsin inhibitor (20.1 kDa), and α-lactalbumin (14.4 kDa) as standards; TD, tracking dye (bromophenol blue). Arrowheads denote bands possibly attributed to the α(95 kDa) and β(38 kDa) subunit of (Na^+,K^+)-ATPase [19]

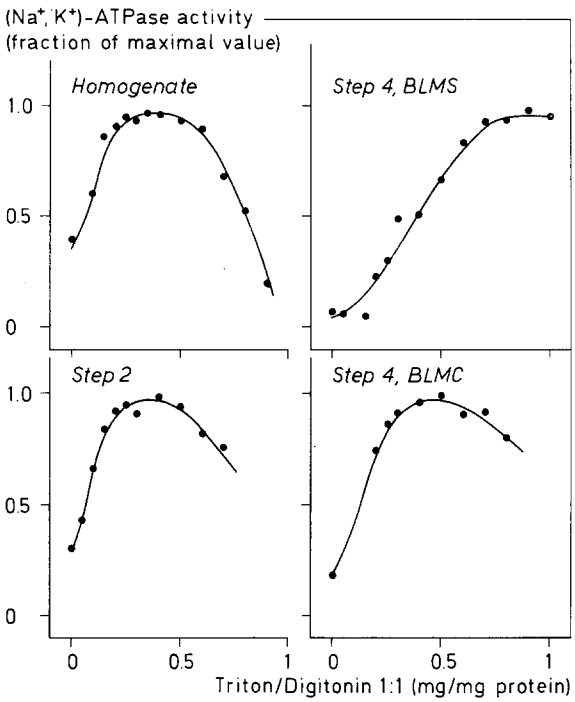

Fig. 6. Expression of latent (Na^+,K^+)-ATPase activity after detergent pretreatment of membranes at different isolation steps. Membrane fractions were purified to the isolation steps indicated (*see* Fig. 3), and preincubated at 1 mg of protein/ml in 10 mM HEPES-Tris, pH 7.4, 250 mM sucrose, for 20 min on ice with varying concentrations of Triton X-100/digitonin, 1:1 (wt/wt), before diluting into the (Na^+,K^+)-ATPase assay mixture. Specific activities were determined under standard assay conditions. The data are averaged from three different batches of membranes and normalized to maximal activity

lipid content of the membrane fractions in the course of purification.

The large increase of ouabain-sensitive (Na^+,K^+)-ATPase activity after preincubation with various leak-producing agents (Table 5) revealed that plasma membranes were largely sealed in both fractions (Table 6). Osmotic shock was slightly less effective in demasking latent (Na^+,K^+)-ATPase activity than detergents suggesting some direct activation of (Na^+,K^+)-ATPase under the experimental conditions used. However, overestimation of the fraction of sealed vesicles introduced by this direct activation is <4%.

Membrane sidedness of sealed vesicles was estimated by measuring latent (Na^+,K^+)-ATPase following trypsin treatment of membrane fractions. Examples of such determinations are given for BLMS and BLMC in Fig. 7 and are summarized in Table 6. In this procedure, membrane fractions were pretreated with trypsin for 10 min just prior to the determination of (Na^+,K^+)-ATPase activity. This incubation time was found to be sufficient (upper curve in Fig. 7) to inactivate that fraction of (Na^+,K^+)-ATPase whose cytoplasmic portion is accessible to trypsin, i.e., inside-out vesicles, leaky vesicles and membrane sheets. The trypsin-insensitive fraction expressed by detergent treatment refers to right side-out plasma membrane vesicles. By these criteria, the vesicle configuration in the BLMS and BLMC fraction approximates a sealed right side-out : sealed inside-out : leaky ratio of 2 : 1 : 1.

Osmotic Properties

Isotope equilibrium space analysis and stopped-flow light scattering experiments indicate that the isolated membrane vesicles are osmotically active.

Table 5. Effect of several treatments on (Na^+,K^+)-ATPase activity of purified membrane fractions[a]

Treatment	BLMS		BLMC	
	Range of maximum activity[b]	(Na^+,K^+)-ATPase (μmol P_i/mg · hr)	Range of maximum activity	(Na^+,K^+)-ATPase (μmol P_i/mg · hr)
None		6.5 ± 3 (8)		2.1 ± 1 (9)
Triton X-100/Digitonin[c] (mg/mg protein)	0.7 – (>1.0)	43 ± 7 (9)	0.4 – 0.6	11 ± 3 (7)
SDS (mg/mg protein)	0.35 – 0.45	44 ± 4 (7)	0.25 – 0.35	13 ± 3 (4)
Alamethicin (mg/mg protein)	0.4 – 0.6	41 ± 4 (4)	0.4 – 0.6	10 (1)
Osmotic shock (-fold dilution)	≥50	36 ± 9 (5)	≥50	10 ± 3 (5)

[a] Final purified membrane fractions were pretreated as indicated and assayed for (Na^+,K^+)-ATPase activity under Materials and Methods. Values are the mean (±SD) of triplicate determinations from different batches of membranes given in parentheses.
[b] Based on lower limit of ≥90% of the maximal (Na^+,K^+)-ATPase activity.
[c] Triton X-100 mixed with digitonin on a 1 : 1 (wt/wt) basis.

The apparent D-[1-^{14}C] mannitol equilibrium space with both BLMS and BLMC was inversely proportional to the osmolarity of the extravesicular medium to at least 50% decrease in entrapped radioactivity (Fig. 8). This implies the presence of an osmotically sensitive compartment in both membrane fractions. However, extrapolation to infinite osmolarity indicates also a small (≤8%) binding component of radioactivity as reflected by intercept values slightly above the horizontal axis. The mannitol equilibrium space at isosmotic conditions corrected for that binding component is a measure of the total intravesicular trapped volume. Table 4 gives representative data and shows that, on a protein basis, the trapped volume in the BLMS fraction (0.91 μl/mg) is ≈fourfold higher than in BLMC (0.24 μl/mg).

Additional evidence for the functional integrity of the isolated membrane vesicles was obtained from experiments following time-dependent changes of scattered light intensity upon osmotic perturbation of vesicles. As shown in Fig. 9, the application of an inwardly directed osmotic gradient produced osmotic water efflux, vesicle shrinkage and increase in scattered light intensity. Within experimental error, this process obeyed first-order kinetic with both membrane fractions suggesting a rather homogeneous water permeability and size distribution of the isolated vesicles. The rate constants at 35°C are 2.39 and 2.69 sec^{-1} with BLMS and BLMC, respectively, corresponding to osmotic water permeability coefficients (P_f) of 6 μm/sec.

Transport Capability and Permeability Barrier for Ions

Both plasma membrane fractions are capable of energized K^+($^{86}Rb^+$) transport, which is inhibited by cardiac glycosides. As shown in Fig. 10, ATP reduces the K^+ content of the vesicles to ≈75% of equilibrium in the absence of ATP as expected for an operating (Na^+,K^+) pump facing the phosphorylation site to the extravesicular medium, i.e., in inside-out vesicles. The amount of K^+ pumped out reached a steady-state level within 3 min resulting from outward K^+ transport and inward K^+ backdiffusion. BLMS exhibited a ≈fourfold larger capacity than BLMC (Table 7). Assuming ≈1/3 of sealed vesicles being of the inside-out configuration (Table 6), a K^+ concentration gradient was generated in

Table 6. Integrity and sidedness of basolateral membrane vesicles from rabbit distal colon epithelium[a]

	(Na^+,K^+)-ATPase	
	Latency	Tryptic sensitivity
	% vesicle in each orientation	
BLMS		
Sealed	84 ± 8 (9)	
Right side-out		58 ± 5 (4)
Inside-out		[26]
Leaky	15 ± 7 (9)	
BLMC		
Sealed	82 ± 5 (7)	
Right side-out		53 ± 10 (5)
Inside-out		[29]
Leaky	18 ± 5 (7)	

[a] The quantitation of leaky and sealed right side-out or inside-out membrane vesicles was based on latency (*see* Fig. 6 and Table 5) and tryptic sensitivity (*see* Fig. 7) of (Na^+,K^+)-ATPase activity. The values reported are the mean ± SD, for the number of determinations on different membrane preparations shown in parentheses. Values in brackets were calculated by the difference from the total percentage of sealed vesicles.

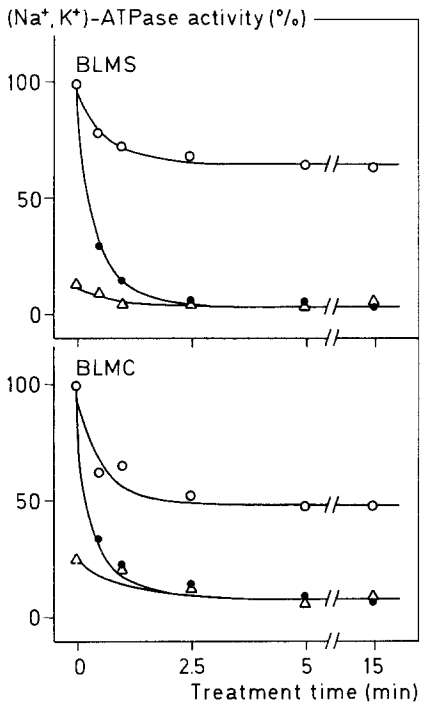

Fig. 7. Trypsin sensitivity of (Na^+,K^+)-ATPase activity in the final purified membrane fractions. Aliquots of final (step 4) purified basolateral membranes were incubated at 2 mg of protein/ml in 250 mM sucrose, 1 mg/ml porcine trypsin (Sigma T-0134), 5 mM HEPES-Tris, pH 7.4, at 25°C. At the indicated time points, proteolysis was stopped by the addition of soybean trypsin inhibitor (final 2.5 mg/ml). In controls ($t = 0$), the order of addition of trypsin and the inhibitor was reversed. (Na^+,K^+)-ATPase activity was determined in the absence (○) or presence (●) of optimized detergent concentrations (*see* Table 5 and Materials and Methods). In a separate experiment, membranes were permeabilized by 5-min preincubation with detergent prior to trypsin treatment and then assayed for (Na^+,K^+)-ATPase activity (△) without further addition of detergent. The data are the average of duplicate determinations for two different batches of membrane fractions and are normalized to maximal (Na^+,K^+)-ATPase activity, i.e., enzyme activity in the presence of detergent with trypsin-untreated membranes (>40 and >10 μmol P_i/mg · hr, for BLMS and BLMC, respectively)

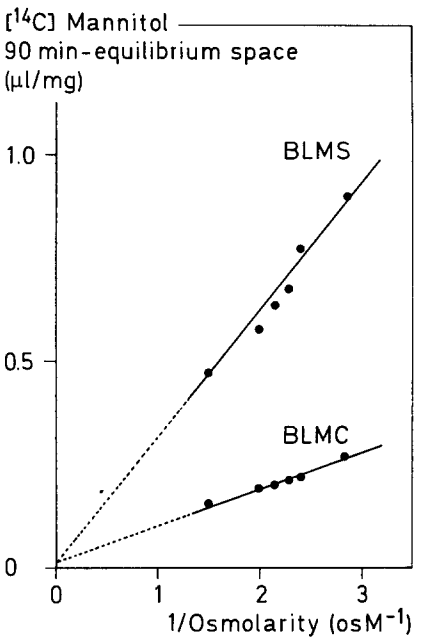

Fig. 8. Relationship of [^{14}C] mannitol equilibrium space to medium osmolarity. Equilibrium uptake (90 min) of D-[1-^{14}C] mannitol in final purified membrane fractions was determined in the presence of increasing amounts of raffinose added to the uptake medium (*see* Materials and Methods). The isotopic content of vesicles was taken as measure of the total apparent space, converted into unit entrapped volume/mg of protein. Data are the average of two different experiments and were fitted to a straight line by linear regression analysis. The entrapped radioactivity at infinite osmolarity, i.e., the extrapolated (dotted line) ordinate intercept represents 0.9% (BLMS) and 8% (BLMC) of the isotopic content at isosmotic ($osM^{-1} = 2.86$) conditions and reflects trapping of the label in an osmotically inactive space

inside-out vesicles, which was four to fivefold higher extravesicular, i.e., a K^+ uphill transport is realized. Digitoxin, a lipid-soluble cardiac-glycoside [14] completely inhibited the ATP-driven K^+ exit (Table 7). On the other hand, ouabain, a membrane-impermeant [14] cardiac-glycoside, had no significant effect at concentrations sufficient to suppress the (Na^+,K^+)-ATPase activity of nonvesicular preparations. These observations are consistent with the known characteristics of the (Na^+,K^+) pump [19] and are a strong indication for the presence of sealed inside-out vesicles in both membrane fractions.

Discussion

The analytical subfractionation of total mucosal scrapings of rabbit distal colon epithelium shows a bimodal distribution of basolateral plasma membranes on a continuous density gradient (Fig. 2). This may be due to either the existence of segregated domains on a single cell type and/or multiple membrane populations, each from different cell types. In fact, mammalian colon is a heterogeneous tissue [6, 36] comprised of a flat surface epithelium containing primarily mature columnar (absorptive) epithelial cells and numerous crypts lined by a single layer of immature apically vacuolated epithelial cells (proposed to function in secretion), goblet (mucus-secreting cells), and few argentaffin (enteroendocrine) cells; the goblet cells comprise a ≈25% [6, 38] component of colonic crypts.

It should be noted, however, that isopycnic fractionation of basolateral membranes obtained from isolated surface epithelial cells revealed only a

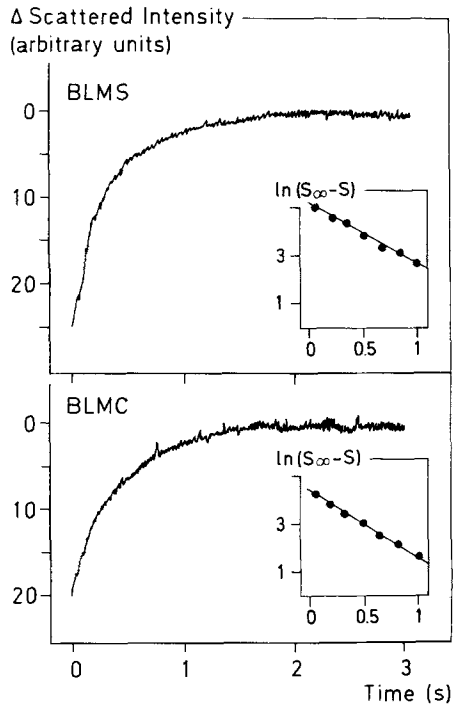

Fig. 9. Osmotic water permeation of basolateral membranes from rabbit distal colon epithelium monitored by light scattering. Membrane vesicles were purified to the final stage and prepared in 100 mM mannitol, 2 mM $MgCl_2$, 5 mM HEPES-Tris, pH 7.4. Aliquots of BLMS (top) and BLMC (bottom) were rapidly mixed with equal volumes of sample buffer containing 200 mM mannitol; final protein, 0.4 mg/ml. Changes in light scatter intensity upon shrinkage of vesicles was followed with time at 35°C by a stopped-flow spectrophotometer system (*see* Materials and Methods). Each curve represents the signal average of four (BLMS) and 12 (BLMC) successive determinations under identical conditions. Inset: first-order replot of the signal change under hyperosmotic conditions determined from, S, the scattered light intensity at time t corrected for the isotonic response, and $S\infty$, the limiting scatter intensity extrapolated to $t = 0$. The slopes of the regression lines ($r \geq 0.998$) yield rate constants of osmotic water permeation, k, of 2.39 and 2.62 sec^{-1} with BLMS and BLMC, respectively

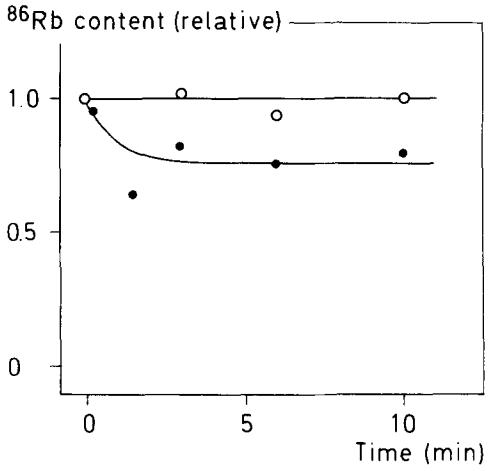

Fig. 10. ATP-dependent potassium outward transport in everted vesicles. Aliquots of the BLMS fraction were preincubated on ice for 3 hr in 5 mM NaCl, 50 mM KCl, 5 mM $MgCl_2$, 2.9 mM EDTA, 5 mM phosphoenolpyruvate, 32 U/ml pyruvat kinase, 50 mM Tris-HCl, pH 7.4, containing 3.5×10^6 cpm/ml of ^{86}Rb. The sample was then temperature equilibrated at 25°C for 30 min. Ion transport was started at zero time by the addition of 3 mM Tris-ATP (filled circles). Controls (open circles) were performed in the absence of ATP. Time-dependent changes of the intravesicular ^{86}Rb content were measured using the Millipore filtration technique. Values are the mean of two experiments normalized to zero time equilibrium ion content of vesicles

Table 7. The effect of cardiac glycosides on ATP-dependent potassium outward transport in everted vesicles[a]

	Potassium content of vesicles (nmol/mg protein)			% control
BLMS control	52	± 6	(5)	100
+ ATP	39	± 5	(5)	75
+ ATP + 0.2 mM ouabain	35		(2)	67
+ ATP + 20 μM digitoxin	49	± 5	(3)	94
BLMC control	13.4	± 2	(4)	100
+ ATP	10.2	± 1.7[b]	(4)	76
+ ATP + 20 μM digitoxin	14.2		(2)	106

[a] Plasma membrane vesicles were equilibrated with ^{86}Rb containing assay medium as described in Fig. 10, except that the indicated cardiac glycosides were included during the last 5 min of preincubation. The reaction was started with the addition of 3 mM Tris-ATP. Ion transport was terminated after 10 min using the vacuum filtration procedure (as under Materials and Methods). Controls were performed in the absence of ATP.

[b] The data represent the mean ± SD for the number of determinations shown in parenthesis, significant ($P < 0.05$) by Student's t test.

single-membrane population. Significantly, its distribution on the density gradient is superimposable to the low density peak seen in the profile obtained with total mucosal scrapings, a diagnostic feature that these membranes derive predominantly from the absorptive surface epithelial cells.

On the other hand, the origin of high density basolateral membranes seems to be the crypt region since, after fractionation of colonic crypts (i.e., mucosal scrapings after removal of the surface cell layer), a substantial increase in the amount of membranes in the high density region of the gradient is observed. However, it should be kept in mind that two major cell types predominate in the secretory crypt region, immature apically vacuolated epithelial cells and goblet cells in a ratio of approximately 3 : 1 [6, 38]. Thus, on the basis of (Na^+,K^+)-ATPase activity as a marker, we would expect the majority of high density basolateral plasma membranes originating from the immature epithelial cells. The pri-

mary function of these cells is electrolyte secretion [38] expecting a rather high (Na^+,K^+)-ATPase content. By contrast, mucus-secreting cells contain relatively low (Na^+,K^+)-ATPase activity [7]. Based on these results, it was possible for the first time to develop a preparative scale purification procedure for isolating sealed basolateral plasma membrane vesicles from both surface and crypt cells of the distal colon mucosa. Judging from transmission electron microscopy studies and marker enzyme analysis, the final membrane fractions are highly enriched in basolateral membranes. The relative specific activity ratio of (Na^+,K^+)-ATPase, a marker for the basolateral plasma membrane of rabbit distal colon epithelium [32], was 34- and ninefold over the crude homogenate with membranes from surface and crypt cells, respectively. However, it should be noted that in the distal colon mucosa, approximately 2/3 of the total (Na^+,K^+)-ATPase activity is associated with surface epithelial cells and only 1/3 with crypt cells (Fig. 1). Assuming similar proportions in homogenates of total mucosal scrapings and given the 34- and ninefold enrichment in (Na^+,K^+)-ATPase activity, we estimate that surface and crypt cell-derived basolateral membranes have been purified 51- and 27-fold with respect to the crude homogenate and that they represent at most 2 and 3.7% of the total protein, respectively. In general, the pattern of marker enrichments confirmed the qualitative conclusions reached from transmission electron micrographs suggesting only minor contamination of the isolated plasma membrane fractions by subcellular organelles.

Methodology based on latency and tryptic sensitivity of (Na^+,K^+)-ATPase activity indicates that the plasma membrane preparation described in this report contains vesicles in the sealed right-side out : sealed inside-out : leaky configuration in a proportion of approximately 2 : 1 : 1. In addition, the vesicle hypothesis was further supported by studies on their functional integrity including osmotic water permeation and ion transport capability both passive- and ATP-energized or ion-gradient driven.

In terms of osmotic water permeation, the basic mechanism observed with basolateral membrane vesicles of rabbit distal colon epithelium seems to be a nonfacilitated, lipid-mediated pathway as indicated by the very low osmotic permeability coefficient of $P_f = 6.1$ μm/sec at 35°C, which is within the range of that obtained for gastric vesicles [29]. For comparison, the corresponding values in small intestinal and renal cortex plasma membranes are, respectively, one and two orders of magnitude higher [16].

The plasma membrane preparations are capable of ATP-energized K^+ transport via (Na^+,K^+) pump as reported here, as well as accumulation of Ca^{2+} ions via the Ca^{2+} pump present in either (BLMS and BLMC) purified fraction (*in preparation*). Each characteristic indicates both a permeability barrier for ions allowing build-up of ion gradients and accessibility of the cytoplasmic membrane face for ATP and, therefore, reflects the presence of sealed inside-out vesicles.

Both vesicle fractions BLMS and BLMC have been shown to effectively generate outward uphill potassium ion gradients, a process that is energized by ATP and inhibited by the membrane-permeant cardiac-glycoside digitoxin. These characteristics are consistent with the activity of a (Na^+,K^+) pump operating in everted plasma membrane vesicles. It should be stressed that the magnitude of potassium ion gradients established at steady-state conditions was estimated to be only four- to fivefold, which is considerably lower than in intact epithelial cells, perhaps reflecting suboptimal experimental conditions, inaccuracies in estimating the proportion of right side-out to inside-out vesicles, and for a rather high rate of backdiffusion due to an intrinsic high permeability of this membrane to potassium. Indeed, electrophysiological studies obtained with intact epithelia indicate a high potassium permeability of the basolateral membrane of rabbit distal colon epithelia cells [40]. Flux experiments performed with vesicles revealed distinct types of potassium channels being present in both fractions BLMS and BLMC (*in preparation*). In mammalian colon, crypt cells are progenitors of the surface cells [6] and, as they move to the surface of the mucosa, their ability of electrolyte and fluid secretion is seemingly lost while absorption capability develops [38]. However, it is as yet unresolved whether the ion transport systems in the basolateral domain of surface and crypt epithelial cells are differently expressed and how they are controlled and modulated to allow rapid transcellular electrolyte transport without perturbing cell-volume and cytosolic-ion activities. Highly purified basolateral membrane vesicles are now becoming available to address these questions. As shown herein, and in the accompanying article, they represent an excellent in vitro system for studies of ion permeation as it appears that they are largely sealed and retain important function properties of the intact cell membrane. Together with apical membrane vesicles [20], they provide a context for interpreting molecular characteristics and regulatory aspects of both absorptive and secretory transcellular ion permeation in the distal colon epithelium.

We thank Prof. Dr. G. Borst Pauwels for kindly providing us the fluorescence polarization supply, Dr. Helene Wiener for performing cytological examinations, Dr. W. Eling for help and advice in histological examinations, Mrs. Gertrude Hellman for

performing SDS gel electrophoresis, M. van Heeswijk for helping in stopped-flow experiments, Dr. G. Eggberink for kindly providing the stereology counting device and M. de Jong for expert technical assistance. We gratefully acknowledge the secretarial and editorial assistance by Mrs. S. Engels.

H.W. was an Erwin Schrödinger Fellow, J 0169 B, Fonds zur Förderung der Wissenschaftlichen Forschung, and was supported by the Austrian-Netherlands scientist exchange program.

References

1. Allain, C.C., Poon, L.S., Chan, C.S.G., Richmond, W., Fu, P.C. 1974. Enzymatic determination of total serum cholesterol. *Clin. Chem.* **20:**470–475
2. Bonting, S.L., Caravaggio, L.L. 1963. Studies on Na,K-activated ATPase. Correlation of enzyme activity with cation flux in tissues. *Arch. Biochem. Biophys.* **101:**37–46
3. Brasitus, T.A., Keresztes, R.S. 1983. Isolation and partial characterization of basolateral membranes from rat proximal colonic epithelial cells. *Biochim. Biophys. Acta* **728:**11–19
4. Brasitus, T.A., Keresztes, R.S. 1984. Protein-lipid interactions in antipodal plasma membranes of rat colonocytes. *Biochim. Biophys. Acta* **773:**290–300
5. Broekhuyse, R.M. 1968. Phospholipids in tissues of the eye. *Biochim. Biophys. Acta* **152:**307–315
6. Chang, W.L.L., Leblond, C.P. 1971. Renewal of the epithelium in the descending colon of the mouse. A presence of three cell populations: Vacuolated columna, mucuous and argentafin. *Am. J. Anat.* **131:**73–100
7. Culp, D.J., Wolosin, J.M., Soll, A.H., Forte, J.G. 1983. Muscarinic receptors and granylate cyclase in mammalian gastric glandular cells. *Am. J. Physiol.* **245:**G760–B768
8. Drenth, E.H.S., Klompmakers, A.A., Bonting, S.L., Daemen, F.J.M. 1981. Transbilayer distribution of phospholipid fatty acyl chains in photoreceptor membrane. *Biochim. Biophys. Acta* **641:**377–385
9. Folch, J., Lees, M., Stanley, G.H.S. 1957. A simple method for the isolation and purification of total lipids from animal tissues. *Biol. Chem.* **226:**497–509
10. Forbush, B., III. 1982. Characterization of right-side-out membrane vesicles rich in (Na^+,K^+)-ATPase and isolated from dog kidney outer medulla. *J. Biol. Chem.* **257:**12678–12684
11. Frizzell, R.A., Schultz, S.G. 1979. Models of electrolyte absorption and secretion by gastro intestinal epithelia. *Int. Rev. Physiol.* **19:**205–222
12. Geiger, B. 1983. Membrane-cytoskeleton interaction. *Biochim. Biophys. Acta* **737:**305–341
13. Giotta, G.J. 1975. Native Na^+/K^+ dependent adenosine triphosphatase has two trypsin sensitive sites. *J. Biol. Chem.* **250:**5159–5164
14. Greenberger, N.J., Mac Dermott, R.P., Martin, J.F., Dutta, S. 1969. Intestinal absorption of 6 ^{3}H-labeled digitalis glucoside in rat and guinea pigs. *J. Pharmacol. Exp. Ther.* **167:**265–237
15. Gustin, M.C., Goodman, D.B.P. 1981. Isolation of the brush-border membrane from the rabbit descending colon epithelium. *J. Biol. Chem.* **256:**10651–10656
16. Heeswijk, M.P.E. van, Os, C.H. van. 1986. Osmotic water permeabilities of brush border and basolateral membrane vesicles from rat renal cortex and small intestine. *J. Membrane Biol.* **92:**183–193
17. Hübscher, G., West, G.R. 1965. Specific assays of some phosphatases in subcellular fractions of small intestinal mucosa. *Nature (London)* **205:**799–800
18. Jackson, R.J., Stewart, H.B., Sachs, G. 1977. Isolation and purification of normal and malignant colonic plasma membranes. *Cancer* **40:**2487–2496
19. Jørgensen, P.L. 1982. Mechanism of the Na^+,K^+-pump. Protein structure and conformations of the pure (Na^+,K^+)-ATPase. *Biochim. Biophys. Acta* **694:**27–68
20. Kaunitz, J.D., Sachs, G. 1986. Identification of a vanadate-sensitive potassium-dependent proton pump from rabbit colon. *J. Biol. Chem.* **261:**14005–14010
21. Laemmli, U.K. 1970. Cleavage of structural proteins during assembly of the head of bacteriophage T_4. *Nature (London)* **227:**680–685
22. Meldolesi, J., Jamieson, J.D., Palade, G.E. 1971. Composition of cellular membranes in the pancreas of the guinea pig: III. Enzymatic activities. *J. Cell Biol.* **49:**150–158
23. Michell, R.H., Karnovsky, M.J., Karnovsky, M.C. 1970. The distributions of some granule associated enzymes in guinea pig polymorphonuclear leucocytes. *Biochem. J.* **116:**207–216
24. Mircheff, A.K., Lu, C.C. 1984. A map of membrane populations isolated from rat exorbital gland. *Am. J. Physiol.* **247:**G651–G661
25. Mircheff, A.K., Wright, E.M. 1976. Analytical isolation of plasma membranes of intestinal epithelial cells: Identification of Na,K-ATPase rich membranes and the distribution of enzyme activities. *J. Membrane Biol.* **28:**309–333
26. Pennington, R.J. 1961. Biochemistry of dystrophic muscle (mitochondrial succinate tetrazolium reductase and adenosine triphosphatase). *Biochem. J.* **80:**649–654
27. Peterson, G.L., Hokin, L.E. 1981. Molecular weight and stoichiometry of the sodium and potassium activated adenosine triphosphatase subunits. *J. Biol. Chem.* **256:**3751–3761
28. Porteous, J.W., Clark, B. 1965. The isolation and characterization of subcellular components of the epithelial cells of rabbit small intestine. *Biochem. J.* **96:**159–171
29. Rabon, E., Takeguchi, N., Sachs, G. 1980. Water and salt permeability of gastric vesicles. *J. Membrane Biol.* **53:**109–117
30. Roufougalis, B.D. 1971. Determination of inorganic phosphate in the presence of interfering amines and nonionic detergents. *Anal. Biochem.* **44:**325–328
31. Sacktor, B. 1977. Transport in membrane vesicles isolated from the mammalian kidney and intestine. *Curr. Top. Bioenerg.* **6:**39–81
32. Schultz, S.G. 1984. A cellular model for active sodium absorption by mammalian colon. *Annu. Rev. Physiol.* **46:**435–451
33. Seiler, S., Fleischer, S. 1982. Isolation of plasma membrane vesicles from rabbit skeletal muscle and their use in ion transport studies. *J. Biol. Chem.* **257:**13862–13871
34. Shinitzky, M., Barenholz, Y. 1978. Fluidity parameters of lipid regions determined by fluorescence polarization. *Biochim. Biophys. Acta* **515:**367–394
35. Sottocasa, G.L., Kuylenstierna, B., Ernster, L., Bergstrand, A. 1967. An electron transport system in mitochondrial outer membrane. *J. Cell Biol.* **32:**415–438
36. Specian, R.D., Neutra, M.R. 1980. Mechanism of rapid mucus secretion in goblet cells stimulated by acetylcholine. *J. Cell Biol.* **85:**626–640
37. Stieger, B., Marxer, A., Hauri, H.-P. 1986. Isolation of brush-border membranes from rat and rabbit colonocytes. Is alkaline phosphatase a marker enzyme? *J. Membrane Biol.* **91:**19–31

38. Welsh, M.J., Smith, P.L., Fromm, M., Frizzell, R.A. 1982. Crypts are the site of intestinal fluid and electrolyte secretion. *Science* **218:**1219–1221
39. Wiener, H. 1986. Heterogeneity of dog liver glutathione S-transferases. Evidence for a unique temperature dependence of the catalytic process. *Eur. J. Biochem.* **157:**351–363
40. Wills, N.K. 1984. Mechanisms of ion transport by the mammalian colon revealed by frequency domain analysis techniques. *Curr. Top. Membr. Transp.* **20:**61–85
41. Wills, N.K., Lewis, S.A., Eaton, D.C. 1979. Active and passive properties of rabbit descending colon: A microelectrode and nystatin study. *J. Membrane Biol.* **45:**81–108
42. Wills, N.K., Zweifach, A. 1987. Recent advances in the characterization of epithelial ionic channels. *Biochim. Biophys. Acta* **906:**1–31
43. Yamato, S., Sahara, I., Sugihara, H., Shimada, K. 1986. Spectrophotometric determination of inorganic phosphate in the presence of thiol compounds. *Anal. Biochem.* **158:**268–271
44. Yonetani, T. 1965. Studies on cytochrome *c* peroxidase. *J. Biol. Chem.* **240:**4509–4514

Received 14 November 1988; revised 30 March 1989